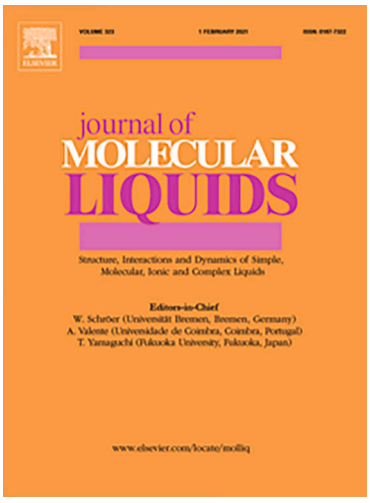

An efficient initiator system containing $AlCl_3$ and supported ionic-liquid for the synthesis of conventional grade polyisobutylene in mild conditions

Saleh Yousefi, Naeimeh Bahri-Laleh, Mehdi Nekoomanesh, Mehrsa Emami, Samahe Sadjadi, Seyed Amin Mirmohammadi, Michele Tomasini, Eduard Bardají, Albert Poater

PII: S0167-7322(22)01920-1
DOI: https://doi.org/10.1016/j.molliq.2022.120381
Reference: MOLLIQ 120381

To appear in: *Journal of Molecular Liquids*

Received Date: 23 May 2022
Revised Date: 24 July 2022
Accepted Date: 12 September 2022

Please cite this article as: S. Yousefi, N. Bahri-Laleh, M. Nekoomanesh, M. Emami, S. Sadjadi, S. Amin Mirmohammadi, M. Tomasini, E. Bardají, A. Poater, An efficient initiator system containing $AlCl_3$ and supported ionic-liquid for the synthesis of conventional grade polyisobutylene in mild conditions, *Journal of Molecular Liquids* (2022), doi: https://doi.org/10.1016/j.molliq.2022.120381

An efficient initiator system containing $AlCl_3$ and supported ionic-liquid for the synthesis of conventional grade polyisobutylene in mild conditions

Saleh Yousefi[1], Naeimeh Bahri-Laleh[1*], Mehdi Nekoomanesh[1], Mehrsa Emami[1], Samahe Sadjadi[2*], Seyed Amin Mirmohammadi[3], Michele Tomasini[4,5], Eduard Bardají[5], Albert Poater[5*]

[1] *Polymerization Engineering Department, Iran Polymer and Petrochemical Institute (IPPI), P.O. Box 14965/115, Tehran, Iran. E-mail: n.bahri@ippi.ac.ir*

[2] *Gas Conversion Department, Faculty of Petrochemicals, Iran Polymer and Petrochemical Institute, PO Box 14975-112, Tehran, Iran. E-mail: s.sadjadi@ippi.ac.ir*

[3] *Department of Chemical Engineering, Central Tehran Branch, Islamic Azad University, Tehran, Iran.*

[4] *Dipartimento di Chimica e Biologia, Università di Salerno, Via Ponte don Melillo, 84084, Fisciano, Italy.*

[5] *Institut de Química Computacional i Catàlisi, Departament de Química, Universitat de Girona, c/ Mª Aurèlia Capmany 69, 17003 Girona, Catalonia, Spain. Email: albert.poater@udg.edu*

Abstract

Ionic liquid based systems are used to facilitate the cationic polymerization of isobutylene to conventional grade polyisobutylene (PIB) using $AlCl_3$ as an initiator. Specifically, the compound 1-butyl-3-methylimidazolium chloride (IL) is employed as a reference system due to its simplicity, as well as the polyionic liquid (PIL), prepared via radical polymerization of 1-butyl-3-vinylimidazolium chloride, and the halloysite clay (Hal) supported ionic liquid (S-IL). The overall

results stated that the designed $AlCl_3$/S-IL initiator system can be used as a safer and greener alternative to the industrially used BF_3 system, in the development of isobutylene polymerizations under mild reaction conditions to conventional grade PIB for viscosity improvement applications. The microstructure and final properties of the as-synthesized PIB was unraveled and compared to Indopole 2100, as a commercial PIB. DFT calculations were performed to understand the different performance of IL and PIL with respect to the S-IL system, and also to show why the catalyst loading for the latter system is lower, as well as to understand how each of the three systems sequesters the catalyst $AlCl_3$. Since the interaction is non-covalent or ionic, in addition to NBO charges, NCI plots were also used.

Keywords: Polyisobutene, polymerization, cationic polymerization, ionic liquid, initiator.

1. Introduction

Generally, during the operation of an engine, some unwanted materials containing soot, sludge, oxidized precursors and other deposit products are formed due to the imperfect combustion/oxidation of the fuel. The so-called unwanted byproducts/deposits result in slow but safe wear of engine parts, which affects engine performance [1,2]. To overcome this problem, additives are generally added to motor lubricant formulations [3,4,5]. The main types of oil additive types are anti-wear agents, detergents, dispersants, and viscosity index (VI) improvers [6].

Since the advent of the lubricant industry, it has been discovered that VI is an important measure of oil quality. It provides an indication of the potential of a lubricant over a wide range of application temperatures. Briefly, small amounts of special polymers dissolved in mineral oil were found to significantly improve its VI characteristic. In this sense, a wide variety of polymers have

been proposed for this application, among which stand out: polymethacrylates, alkylated polystyrene, ethylene-propylene copolymers and terpolymers, hydrogenated polyisoprene, polyisobutylene (PIB), etc. [7,8]. The latter, due to its high thermal stability, exceptional adhesion properties, odorless and nontoxic nature, as well as good chemical and weather resistance, and crack-free carbon residue, have attracted considerable interest among users [9]. Especially, PIB meets the standards properly when targeting low temperature applications. As a result, in some countries, PIB has a monopolistic position in the VI enhancer market [10].

PIB is a type of vinyl polymer, synthesized from the monomer isobutylene (IB) by cationic polymerization. Currently, a wide range of Lewis acid initiators including BF_3, $AlCl_3$, and $TiCl_4$ are employed to synthesize PIBs [11,12]. Alongside the cationic initiator, a second chemical species, called as a co-initiator, is generally used. This species contributes to the chain initiation step, by forming an initiator/co-initiator complex that consequently releases H^+ or R^+ (R is an alkyl group) ion, acting as the main initiator. In addition, during propagation, the co-initiator component is located as a counter-ion in the vicinity of the active site and, by donating electrons to the initiator, affects the microstructure of the polymer chain. Various Lewis bases such as water, alcohols and organic acids are the most common cationic polymerization co-initiators [13].

Among the initiators mentioned, BF_3/co-initiator systems are commonly used in the industrial production of PIB. According to the literature, harsh conditions of (T<-40 °C), with the initator BF_3, are required to prepare suitable PIBs, for the application of viscosity improvers [14]. Providing such a low temperature is costly in industry, and also in the laboratory. It affects the economics and safety of isobutylene polymerization. Increasing the polymerization temperature to room temperature is of great importance among researchers and industrialists. Furthermore, since

BF_3 is a toxic gas that limits its use, replacing it with less hazardous $AlCl_3$, in the isobutylene polymerization has attracted researcher's attention [13,15].

Beyond these, it was certified that ionic liquid compounds, in combination with the initiator $AlCl_3$ [16], motivate a greener process by decreasing the amount of initiator needed (which is extremely corrosive) in the cationic polymerization of α-olefins [7,17,18,19]. In fact, ionic liquids are non-toxic, no-corrosive materials [20,21], which by replacing them as part of the $AlCl_3$ corrosive catalyst, doubles the advantage of the catalytic system used to extend the life of the unit apparatus of production.

On the other hand, to support and enhance the catalytic polymerization, halloysite (Hal) [22,23,24] have been combined here with the $AlCl_3$ catalyst. Hal systems, with a wide range of applications [25,26,27,28], have unique physicochemical properties, with oppositely charged inner and outer surfaces [29,30,31], which facilitate not only covalent interactions, but also non-covalent ones [32,33,34]. This results in applications of Hal based systems for various chemical reactions, from hydrogenation [35,36] and oxidation reactions [37], to the synthesis of organic compounds [38,39] and polymerization [40,41].

Considering the above facts and concerns, this research aims to design new cationic initiator systems that can promote the polymerization of isobutylene under mild reaction conditions and low $AlCl_3$ content. This is achieved by using three types of ionic liquid-based systems, including 1-butyl-3-methylimidazolium chloride, denoted as IL, Hal-supported ionic liquid [42], S-IL, and polyionic liquid, PIL, prepared via a radical polymerization of 1-butyl-3-vinylimidazolium chloride (Scheme 1), together with the initiator $AlCl_3$. After synthesis and optimization of the reaction conditions, the main characteristic of the final PIB product was compared with a commercially available conventional PIB grade, *i.e.* Indopol 2100, in oil upgrading application VI.

2. Experimental

2.1. Reagents

The solvents and reagents required for the synthesis of the ionic liquid based catalytic systems include Hal, (3-chloropropyl) trimethoxysilane (CPTES), diethyl ether, azobisisobutyronitrile (AIBN), methanol, 1-vinyl imidazole, imidazole, 1-methylimidazole, 1-butyl chloride and toluene, and anhydrous $AlCl_3$ (Aldrich, 99.999%), were all provided from Sigma-Aldrich. Isobutylene (>99.0 %) was kindly donated by Bandar Imam petrochemical company, Iran. NaOH and ethanol (purchased from Sigma-Aldrich) were also used in the course of PIB synthesis.

2.2. Synthesis of 1-butyl-3-methylimidazolium chloride: IL

Synthesis of IL has been fulfilled according to previous reports [42]. Briefly, a mixture of 1-butyl chloride (1 mmol) and 1-methylimidazole (1 mmol) in a flask was heated at 70 °C and stirred for 24 h under Ar atmosphere. Upon completion of the process, the viscous product was collected and rinsed with diethyl ether. Subsequently, the purified product, IL, was dried under vacuum (Scheme 1).

2.3. Synthesis of PIL

To synthesize the polymerizable ionic liquid PIL, 1-butyl-3-vinylimidazolium chloride, was first prepared and then polymerized via conventional radical polymerization. More accurately, 1-vinyl imidazole (1 mmol) and 1-butyl chloride (1 mmol) were mixed under Ar atmosphere at 70 °C for 20 h. Then, the obtained viscous liquid was washed with diethyl ether and dried at 60 °C in a vacuum oven. To polymerize the as-prepared monomer, 1-butyl-3-vinylimidazolium chloride (1 g) was transferred to a flask containing toluene (30 mL) and then AIBN (0.03 g) was added. The reaction mixture was then stirred at 80 °C for 4 h under Ar atmosphere. In the end, the product,

named PIL, was collected, rinsed several times with methanol and dried in a vacuum oven at 70 °C, overnight, Scheme 1.

2.4. Synthesis of Hal-supported ionic liquid: S-IL

The synthesis of the Hal-supported ionic liquid was carried out through a three-step procedure. First, Hal outer surface was Cl-functionalized using a known procedure [17]. Typically, a homogeneous suspension of Hal in toluene was prepared by sonicating Hal (2 g) in dry toluene (50 mL) for 15 min (140 W). CPTES (3 mL) was then added to the reaction vessel and the reaction was continued under reflux conditions for 16 h. Finally, the product, Hal-Cl, was separated by centrifugation, rinsed with toluene and dried at 40 °C overnight. In the next step, the as-prepared Hal-Cl was reacted with imidazole to provide Hal-Im. In this context, imidazole (1 g) was dissolved in n-heptane (40 mL) and added to the suspension of Hal-Cl (2 g). The resulting mixture was then stirred at 90 °C overnight. Afterwards, the precipitate was separated, rinsed with n-heptane twice, and dried at 50 °C overnight. In the final step, Hal-Im (2 g) was suspended in n-hexane (40 mL) and then reacted with 1-butyl chloride (1.2 g) under reflux overnight. The product, S-IL, was obtained after washing with n-heptane and drying at 70 °C overnight (Scheme 1).

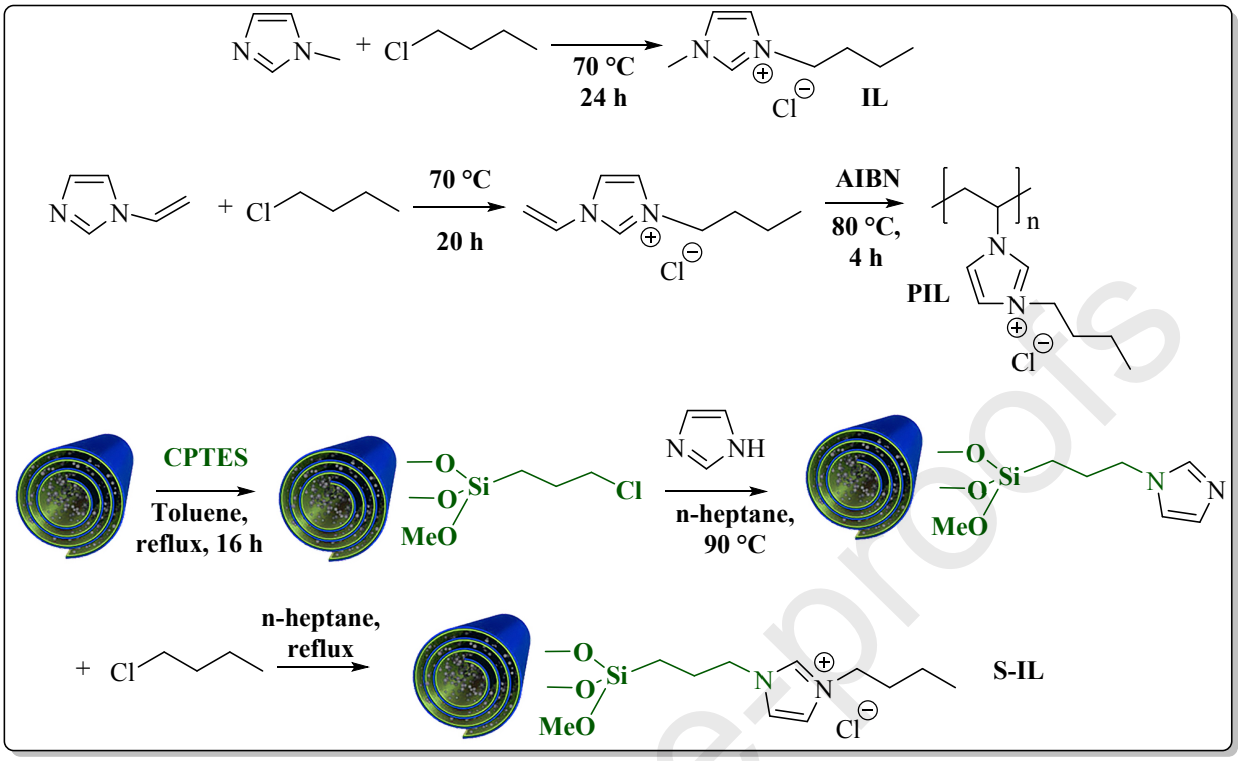

Scheme 1. Employed procedure for the synthesis of IL, PIL and S-IL

2.5. Isobutylene polymerization process

The synthesis of polyisobutenes was conducted by polymerization of isobutene monomer in a 1 L Buchi type stainless steel reactor equipped with a temperature and pressure sensor. Before each experiment, the reactor was purged with argon gas at 100 °C for 30 min. Then, it was cooled to the desired temperature, according to the reaction conditions in Table 1. The initiator composition containing $AlCl_3$ and S-IL, IL and PIL, with a molar ratio of 2:1 (in the case of S-IL, the molar ratio of $AlCl_3$ to S-IL was 1:24 mol/mol) and total amount of almost 1 wt. % of primary monomer weight, ethanol (ethanol/$AlCl_3$=1:2 molar ratio), and 300 g isobutylene monomer were subsequently introduced into the reactor. The reaction was continued for 1 h. The final product was discharged through a valve located at the bottom of the reactor and repeatedly washed using NaOH solution with 5 wt. concentration. PIB purification (removal of water, unreacted monomers

and very low molecular weight polyisobutylene oligomers) was conducted by using rotary evaporation at 150 °C under a vacuum of a 0.8 bar.

2.6. Instruments

To characterize the ionic liquid-based systems, IL, PIL, S-IL and polyisobutenes, the following instruments have been employed: To obtain a better view of the morphology of the synthesized S-IL, transmission electronic microscopy (TEM, Philips100 Kv AMBS) was used. To confirm the successful synthesis of S-PIL, Fourier transform infrared (FTIR) spectra of the final product and Hal were recorded via a PERKIN-ELMER Spectrum 65 using KBr pellet. Siemens, D5000 armed with a Cu Kα radiation was applied to record the X-ray diffraction (XRD) pattern of the S-PIL sample. To estimate the value of organic moiety grafted on the Hal carrier in S-PIL, thermogravimetric analysis (TGA) of the final product was performed on METTLER TOLEDO apparatus with a heating rate of 10 °C/min under O_2 atmosphere. To shed light on the homogeneity of organic moiety binding onto Hal support in S-PIL, elemental mapping analysis was carried out by a MIRA 3 TESCAN-XMU instrument. The textural properties of Hal and the catalyst were measured using BELSORP MINI II, BEL apparatus. ^{1}H and ^{13}C Nuclear Magnetic Resonance ($^{1}HNMR$ and $^{13}CNMR$) spectroscopies were performed on the Bruker DRX 400 MHz instrument in chloroform solvent to estimate the type of unsaturation and microstructure of the synthesized polyisobutenes. The GPC instrument was used to obtain molecular weight and its distribution of the synthesized polymers using the GPC Agilent 1100 instrument in chloroform solvent at a flow rate of 1.0 mL/min. The viscosity increase and viscosity index (VI) of the selected PIB sample were measured according to the D445 and D2270 standards, respectively.

2.7. Computational details

Density Functional Theory (DFT) calculations were performed with the Gaussian16 package [43]. Geometry optimizations were carried out without symmetry constraints via the spin-restricted Kohn-Sham (RKS) formalism and the BP86-D3 functional of Becke and Perdew [44,45] with the Grimme D3 correction term to the electronic energy [46]. The split-valence basis set (Def2-SVP keyword in Gaussian) was used for all atoms [47,48]. Frequency calculations were performed in order to confirm the nature stationary points (minima without imaginary frequencies). Solvent effects were evaluated on the polarizable solvation model (SMD), variation of IEFPCM of Truhlar and co-workers [49], using ethanol as the solvent; employing the B3LYP hybrid GGA functional of Becke-Lee, Parr, and Yang [50,51,52], and the valence triple-zeta polarization basis set (Def2TZVP) to increase the accuracy. In addition, to model the S-IL systems, despite being relatively smaller compared to similar studies with silica based systems [53], we used the Hal model based on three Al and two Si units [54].

3. Results and discussion

3.1. Effect of ionic liquid type on the molecular weight of the synthesized PIBs

Recently, we have reported the impactful ionic liquid on controlling molecular weight and microstructure of synthesized polyalphaolefin type lubricants [55], via cationic systems [56,57]. The promising data obtained encouraged us to extend those experiences into the cationic polymerization of isobutylene monomer to produce low molecular weight PIB, suitable for oil viscosity improver application. In this sense, three different ionic liquid based compounds were prepared: i) IL, ii) PIL, structurally similar or almost identical to IL, but in polymeric form; was actually synthesized by radical polymerization of already prepared ionic liquid preform from vinyl imidazole and butyl chloride, and finally iii) S-IL, synthesized by growth of an ionic liquid on Hal support [58,59,60,61]. The consecutive reactions to synthesize ionic liquid compounds are

illustrated in Scheme 1. Next, we describe the effects of these (poly)/ionic liquids on the catalytic performance of $AlCl_3$/EtOH system and the microstructure of final PIBs.

The synthesized IL, PIL and S-IL together with the $AlCl_3$ initiator were briefly tested in the cationic polymerization of isobutylene, regarding the possibility of preparing conventional grade PIB (with molecular weight between 2500-5000 g/mol) and estimation of their reactivity at high temperatures. Neat $AlCl_3$ was also employed as the blank system. In this regard, the effect of polymerization temperature, as the most important parameter, on the catalytic performance of the designed catalysts was studied, runs 1-4 in Table 1. The amount of initiator dosage was set at 1 wt. % of the initial monomer weight. It is worth mentioning that in the experiments containing ionic liquid compounds, the sum of $AlCl_3$ and the weight of the ionic liquid was used as the initiator dosage. The result implied that under the employed reaction conditions, isobutylene polymerization yield was in the range of 88-90 %. It is noteworthy that the presence of ionic liquid did not alter the polymerization yield and, considerably, high turnovers were acquired in all systems studied. It is worth mentioning that in the case of S-IL at low $AlCl_3$ dosages, *i.e.* 2:1 of the ratio $AlCl_3$:Hal, very low activities were obtained. Therefore, the molar ratio of $AlCl_3$ to S-IL was kept at 24:1 to obtain a reasonable yield. Notably, in the experiments containing IL, PIL and S-IL compounds in the catalytic compositions, the amount of $AlCl_3$ initiator used was almost halved, which affirms the environmentally benign nature of the designed catalyst systems.

Turning to the molecular weight data, it can be deduced that the average molecular weight (M_n) of the synthesized PIB increases in the catalytic systems containing ionic liquid compounds, entries 2-4 in Table 1. This can be due to the stabilization of the carbenium ion (located at the end of the growing polymeric chain) through its interaction with the ionic liquid compounds used. In fact, the highest stabilization effect was observed in the S-IL case, in which the highest molecular

weight of 11,500 g/mol was obtained for the corresponded PIB. In this case, the presence of Hal support, which contains surface hydroxyl groups, may contribute to improvement of $C^{+}\cdots$S-IL (C^{+} is an active part of a growing chain) interactions. In more detail, the GPC curves show some shoulders, which can be assigned to the nature of the active site of the initiators used. Specifically, as demonstrated in Figure 1B-E, by deconvolution of the GPC curves into a weighted sum of three or four Gaussian distribution functions, the number and productivity of each active site is quantified. Consequently, neat $AlCl_3$ provided more heterogeneous PIB chains, with a broader Đ of 3.0 originated from four different active sites (Figure 1B). In this sample, the molecular weights of the first three Flory peaks are less than 8,100 g/mol and these components constitute 84 % of the total peaks. Ionic liquid-based compounds, by the deactivation of some specific active sites, reduce the number of active centers to three (Figure 1C-E) and, consequently, total Đ approaches to a value in the range of 1.7-1.9. Interestingly, the first peak of the GPC curve of PIB of S-IL (Figure 1E) has a higher M_n value (comparing 6,478 with 4,443 and 4,970 g/mol), which is the main reason of the higher molecular weight of polymer of run 1. It means that S-IL, by poisoning some active sites that led to the formation of low molecular weight polymers, affects total molecular weight value. This behavior is almost identical to the characteristic of electron donors in olefin polymerizations using heterogeneous catalysts [62,63,64]. The so called sample would form enough inter-chain entanglement, which is an advantage in conventional grade PIBs. It is worth mentioning that, due to nature of GPC analysis, a ±15 % error in the reported molecular weights is normal, therefore this test was repeated twice for each sample, and almost same results were obtained every time. Considering the higher molecular weight of PIB using the S-IL catalyst, this system was chosen as the best catalyst, and additional experiments were performed to find out the appropriate reaction conditions to obtain the target degree of PIB. Exceptionally, the mentioned

initiator system has the least amount of corrosive $AlCl_3$ in the composition of the designed catalyst (compared to those containing IL and PIL and neat $AlCl_3$), beneficial for the green character of the whole process.

Table 1. Cationic polymerization of isobutylene by $AlCl_3$/EtOH initiator in the presence of the synthesized ionic liquids at different temperatures and times.[2]

Run		Initiator dosage (%)	$AlCl_3$/ionic liquid (g/g)	t (min)	T (°C)	Yield (%)	M_n (g/mol)	Đ[1]
1	$AlCl_3$	1	2.1/0	60	-20	89	3,900	3.0
2	$AlCl_3$/IL	1	1.3/0.8	60	-20	88	10,300	1.9
3	$AlCl_3$/PIL	1	1.2/0.9	60	-20	90	10,900	1.9
4	$AlCl_3$/S-IL	1	1.1/1.0	60	-20	88	11,590	1.7
5	$AlCl_3$/**S-IL**	**1**	1.1/1.0	**60**	**0**	**87**	**4,100**	**2.3**
6	$AlCl_3$/S-IL	1	1.1/1.0	60	20	87	1,500	3.5
7	$AlCl_3$/S-IL	1	1.1/1.0	40	0	80	4,050	2.2
8	$AlCl_3$/S-IL	1	1.1/1.0	20	0	73	4,130	2.4
9	$AlCl_3$/S-IL	0.5	1.1/1.0	60	0	70	6,040	4.4

[1]M_w/M_n , [2]Polymerization conditions: Monomer= 210 g, t= 1 h, EtOH/$AlCl_3$= 0.5 mol/mol.

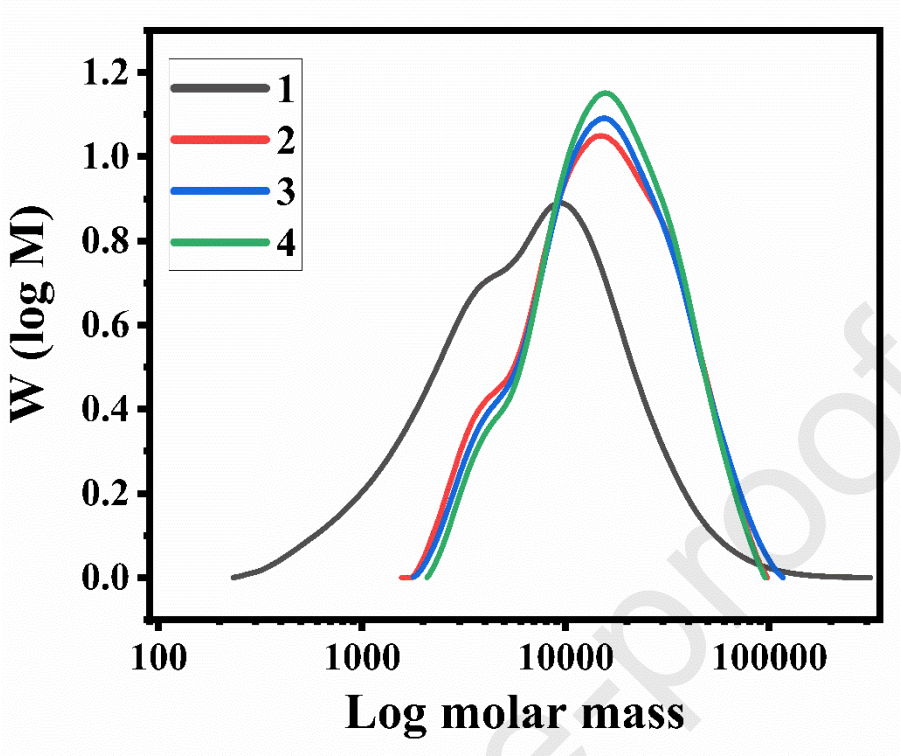

238

239 A

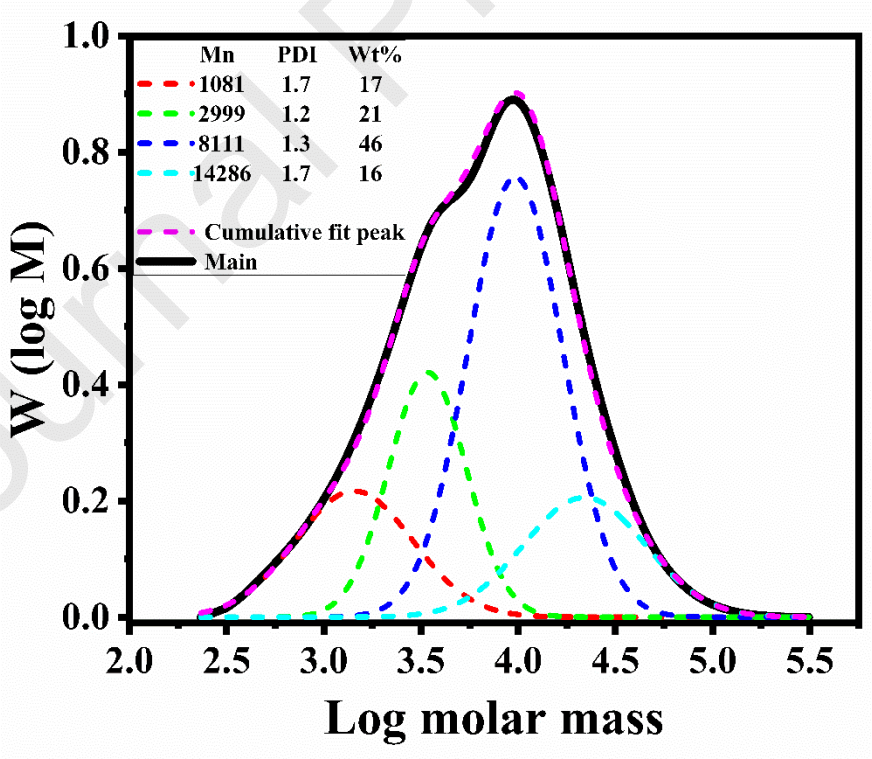

240

241 B

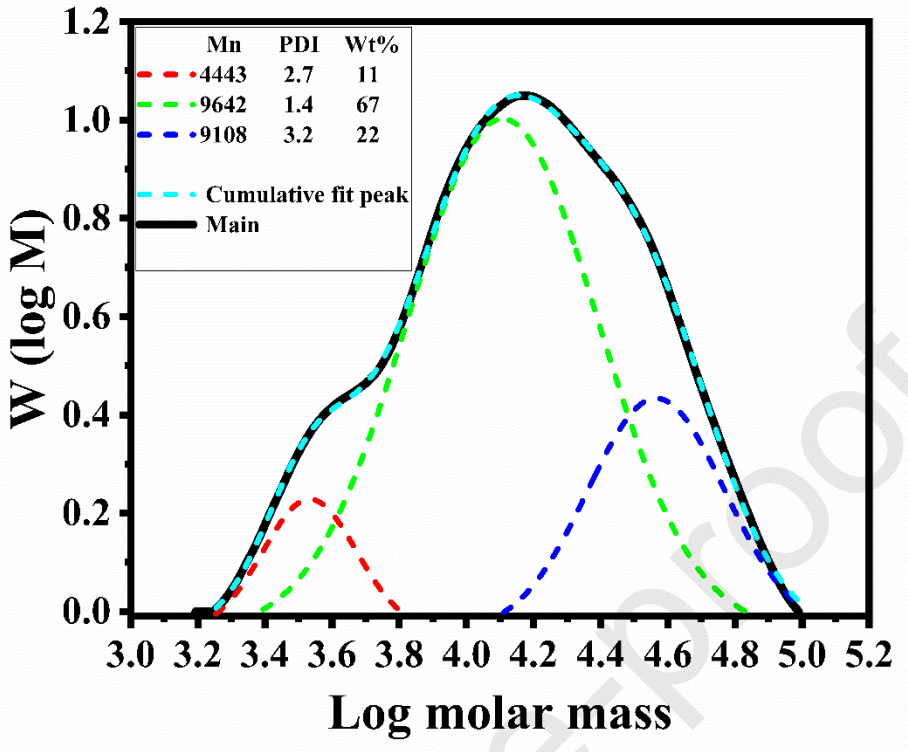
Mn PDI Wt%
4443 2.7 11
9642 1.4 67
9108 3.2 22
Cumulative fit peak
Main
W (log M)
Log molar mass
1.2
1.0
0.8
0.6
0.4
0.2
0.0
3.0 3.2 3.4 3.6 3.8 4.0 4.2 4.4 4.6 4.8 5.0 5.2

C

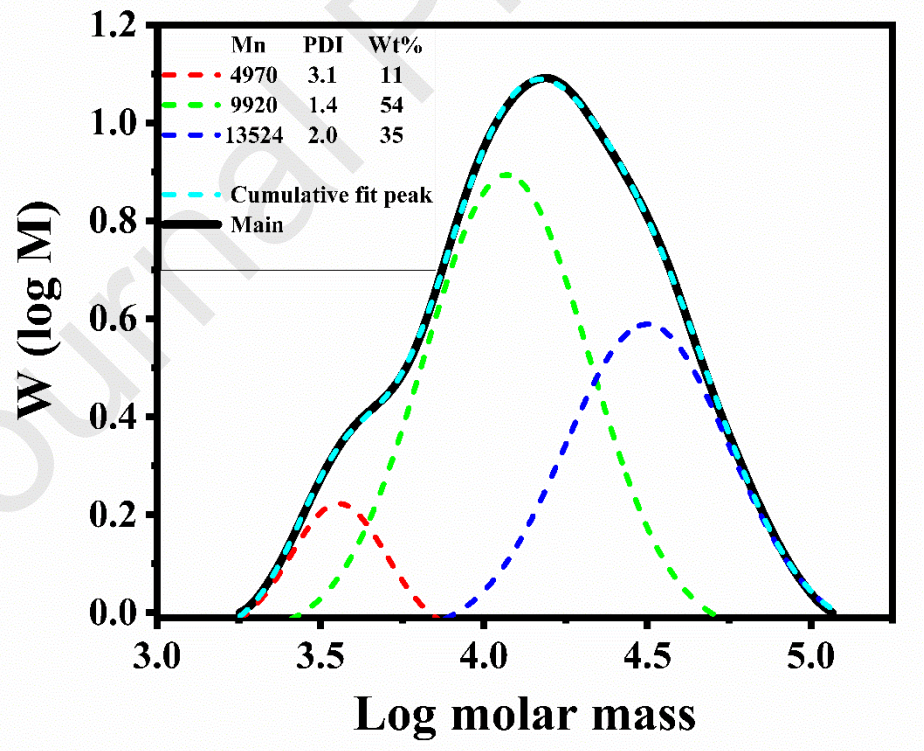
Mn PDI Wt%
4970 3.1 11
9920 1.4 54
13524 2.0 35
Cumulative fit peak
Main
W (log M)
Log molar mass
1.2
1.0
0.8
0.6
0.4
0.2
0.0
3.0 3.5 4.0 4.5 5.0

D

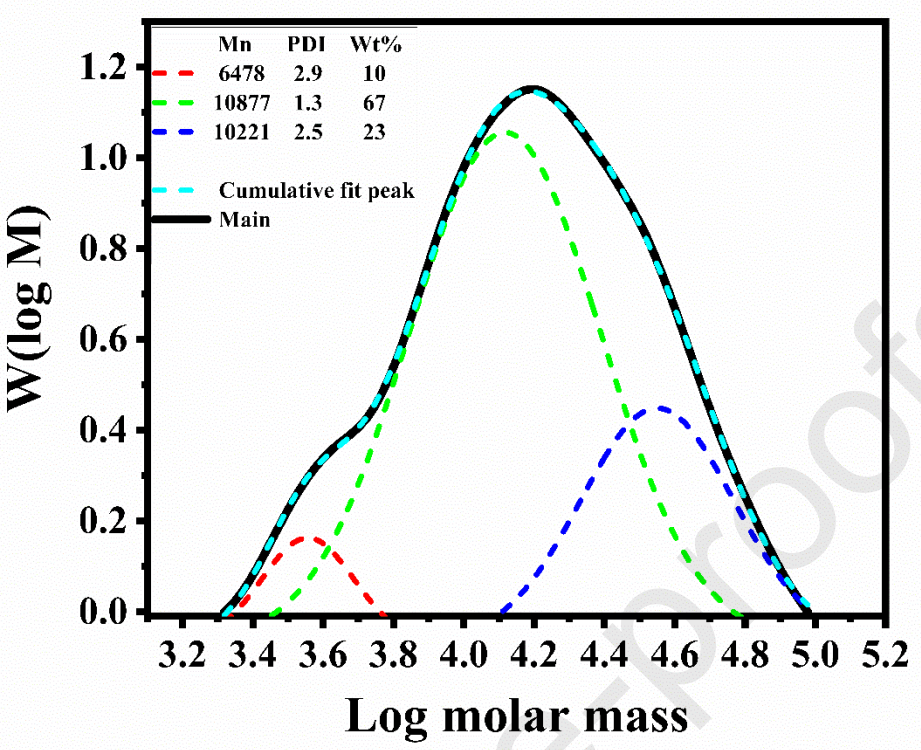

E

Figure 1. A) GPC curves of the synthesized PIBs using different catalytic systems (runs 1-4), and deconvolution of the experimentally measured MMD to a weighted summation of 3-4 lognormal distribution functions for PIBs from B) run 1, C) run 2 and D) run 3 and E) run 4. The characteristics of each distribution including the number average molar mass, polydispersity index and weight fraction are indicated in the inset table.

Next, the effect of temperature was studied by performing the polymerization reaction at different temperatures (-20, 0 and 20 °C) and comparing the molecular weight results. It was inferred that the polymerization temperature has no noticeable effect on the reaction yield. Nevertheless, a sharp decrease in molecular weight was noted with increasing temperature. Indeed, M_n suppressed from 11,900 to 4,100 and 1,500 g/mol by carrying out the reaction at T=-20, 0 and 20 °C. Also, the GPC curve of sample 6 exhibited the highest number of shoulders, indicating the high amount of chain

transfer reactions at high temperature. Considering the molecular weight data, entry 5, with $T_{polymerization}$= 0 °C, was selected as the optimal reaction temperature. To elucidate the effect of time, the polymerization reaction, repeated under the conditions of entry 6, was stopped at t=20 and 40 °C. It was found that the molecular weight does not change with time, however, the polymerization yield reduced considerably from 87 to 80 and 73 %, respectively. Remarkably, the reasonable high conversion of 73 % is achieved at a short polymerization time of 20 min, which confirms the high efficiency of the designed catalyst. In the final stage, the polymerization was carried out at lower initiator dosage of 0.5 wt. % towards the monomer feed. By reducing the initiator dosage, a decrease in productivity (entries 5 and 9, Table 1, 87 % vs 70 %) and sharp increase in M_n (4,100 vs 6,040 g/mol) were observed. Consequently, considering the above experiments, the optimal initiator loading, temperature and time were 1 wt. %, 0 °C and 1 h, respectively. Under these conditions (run 5), suitable PIB for the target application (as a viscosity improver) was provided with a yield of 87 %. It is worth mentioning that the employed reaction conditions and low initiator dosage, pronounced the green character of the employed initiator in performing isobutylene polymerizations under mild reaction conditions. As mentioned above, harsh reaction conditions, *i.e.* T<-40 °C, using corrosive and hazardous BF_3 gas as a cationic initiator, were reported for the production of this type of polymers, in industry [14].

3.2. Microstructure analyses of the synthesized PIBs

Another important parameter of PIBs is the nature of their unsaturated bonds. These bonds are formed as a result of various transfer reaction mechanisms during PIB synthesis. Vinyl hydrogen can be divided into two main groups: exo-olefinic and endo-olefinic types. They have different stabilities and determine the type of PIB as conventional and highly reactive grades. Therefore,

unraveling the type of C=C moieties formed in the structure of the synthesized PIBs is a key factor that determines their durability in high temperature applications.

Next, the type of C=C moieties, such as exo, endo, tri-substituted, tetra-substituted and coupled (Scheme 2) was explored from the ^{1}HNMR spectra of the synthesized PIBs in the region δ = 4.64-5.17 (Figure 2). According to results in Table 2, pure $AlCl_3$ furnishes PIB with a total exo-olefin end group content of 24.3 %. Under the same reaction conditions, however, with different catalyst systems containing IL, PIL and S-IL, the total exo-olefin end group decreases to 6.2, 4.7 and 10.2 %, respectively (runs 2-4, Table 2). The lower exo-olefin end group content is favorable for conventional grade PIB, since it improves the thermal oxidative stability of the polymer for high temperature uses. Actually, it is well accepted that exo olefins are more reactive than endo ones which deteriorates the performance of PIB at high application temperatures [65]. The effect of polymerization temperature on the olefinic type of the resulting PIBs was then analyzed (runs 4-6, Table 2) using the same S-IL containing initiating system. Accordingly, by increasing the temperature from -20 to 0 and 20 °C, the reaction conditions become more severe and consequently, the share of exo olefins minimizes, in accordance with the results of previously published literature [66,67]. Unlike temperature, the time had unfavorable effect on exo content (runs 5, 7 and 8). In fact, decreasing the polymerization time resulted in a dramatic increase of the exo-olefins from 8.9 to 16.4 and 25.2 %, mainly due to the decrease of tri and tetra-substituted fractions. This was correlated to the isomerization of exo-olefins by the polymerization progress [68]. As a final assess, decreasing the $AlCl_3$ initiator dosage did not alter the share of total exo, however, the amount of each vinyl structure varied.

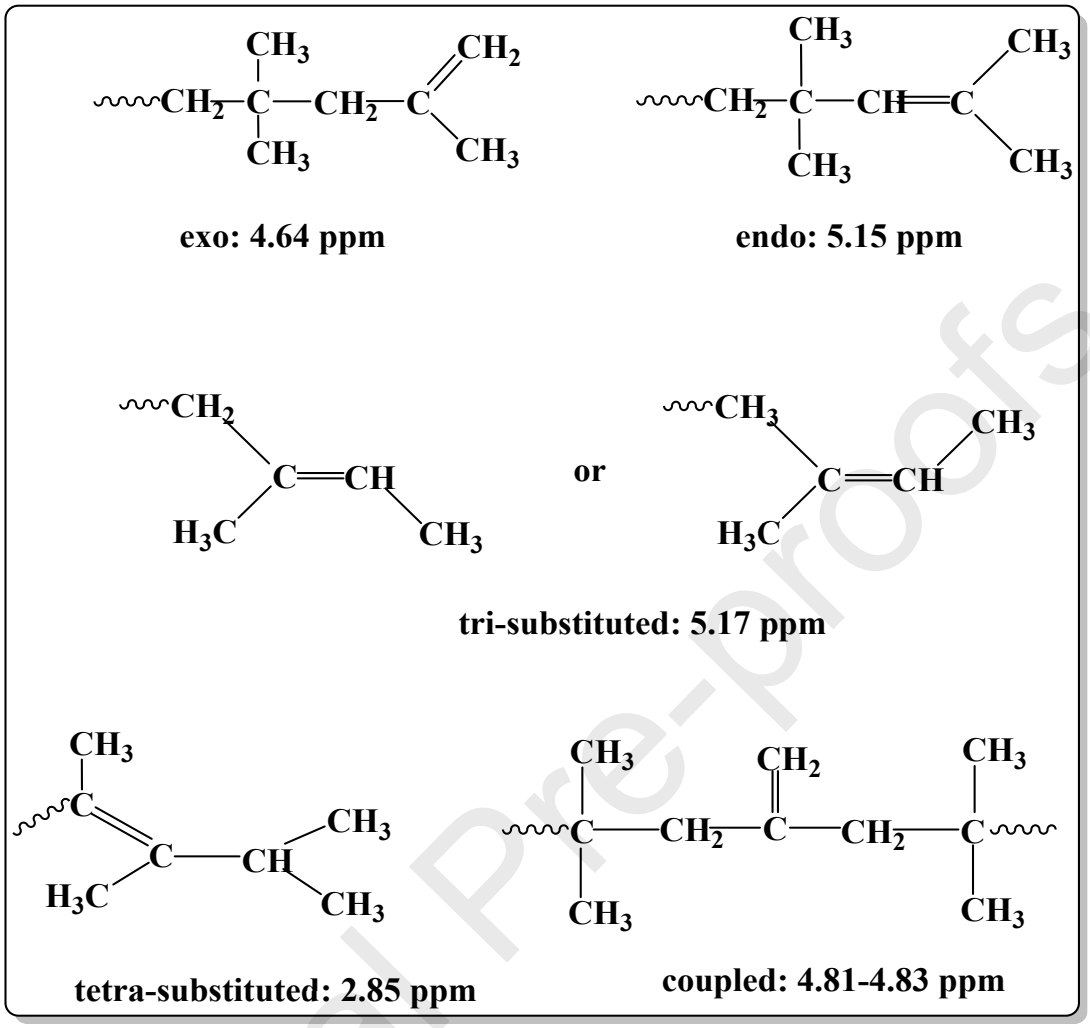

Scheme 2. Various unsaturated C=C double bonds in the structures of PIBs.

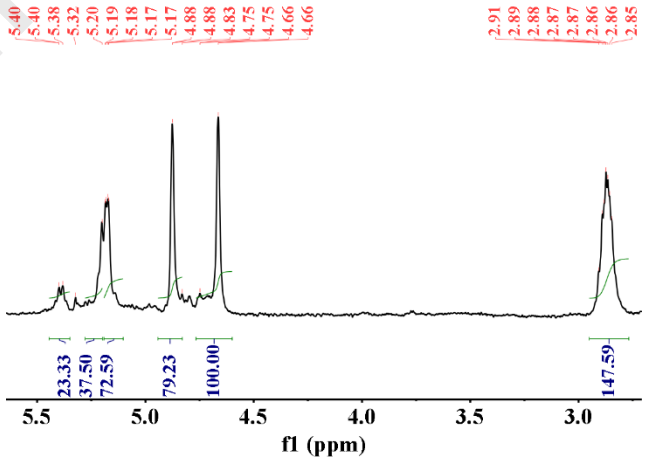

A

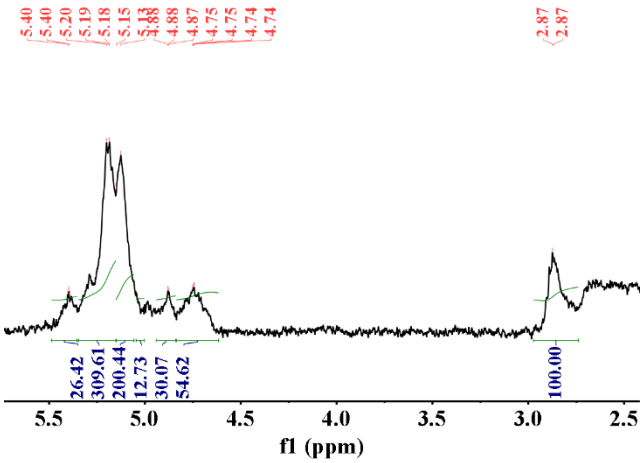
5.40
5.40
5.20
5.19
5.18
5.15
4.88
4.87
4.75
4.74
4.74
2.87
2.87
26.42
309.61
200.44
12.73
30.07
54.62
100.00
5.5
5.0
4.5
4.0
3.5
3.0
2.5
f1 (ppm)

B

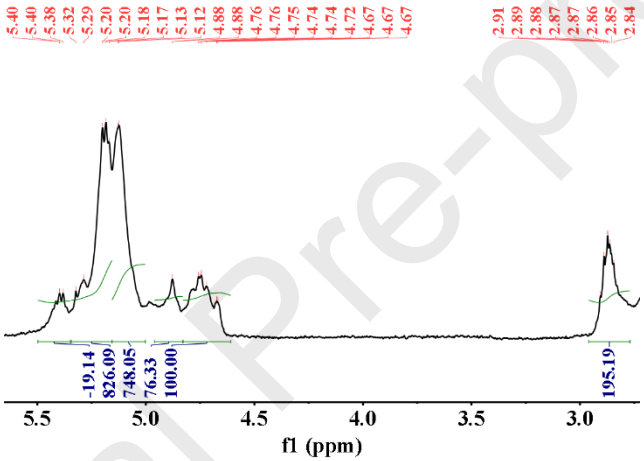
5.40
5.40
5.38
5.32
5.29
5.20
5.20
5.18
5.17
5.13
5.12
4.88
4.88
4.76
4.76
4.75
4.74
4.74
4.72
4.67
4.67
4.67
2.91
2.89
2.88
2.87
2.87
2.86
2.85
2.84
-19.14
826.09
748.05
76.33
100.00
195.19
5.5
5.0
4.5
4.0
3.5
3.0
f1 (ppm)

C

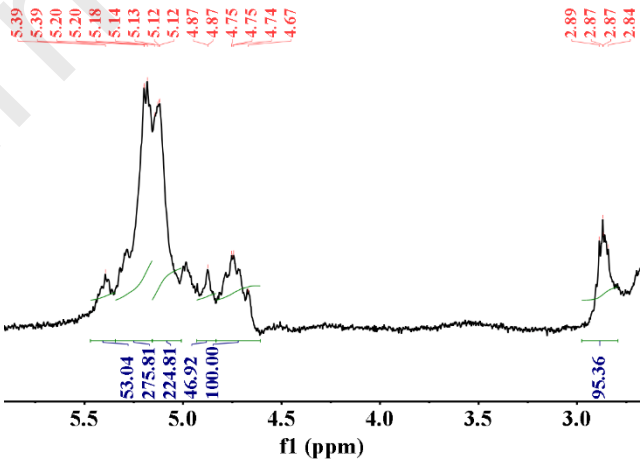
5.39
5.39
5.20
5.20
5.18
5.14
5.13
5.12
5.12
4.87
4.87
4.75
4.75
4.74
4.67
2.89
2.87
2.87
2.84
53.04
275.81
224.81
46.92
100.00
95.36
5.5
5.0
4.5
4.0
3.5
3.0
f1 (ppm)

D

Figure 2. ^{1}HNMR spectra of the synthesized PIBs from catalysts a) $AlCl_3$ (run 1), b) IL (run 2), c) PIL (run 3) and S-IL (run 4).

Table 2. End group distribution of the synthesized PIBs using different polymerization conditions.

Run	Exo (4.64-4.65)	Endo (5.15)	tri-1 (5.17)	tri-2 (5.36)	Tetra (2.85)	Couples (4.81-4.83)	Total exo*
1	**13.6**	**19.5**	**10.0**	**6.2**	**39.9**	**10.7**	24.3
2	**4.0**	**29.5**	**45.6**	**3.8**	**14.8**	**2.2**	6.2
3	**2.7**	**39.9**	**44.0**	**1.0**	**10.4**	**2.0**	4.7
4	**6.9**	**31.1**	**38.2**	**7.4**	**13.2**	**3.3**	10.2
5	**5.5**	**24.1**	**40.6**	**5.9**	**20.5**	**3.4**	8.9
6	**5.6**	**34.6**	**44.1**	**6.2**	**9.4**	**0.1**	5.7
7	**7.8**	**24.6**	**24.1**	**14.5**	**20.4**	**8.6**	16.4
8	**19.3**	**33.0**	**21.2**	**11.8**	**8.8**	**6.0**	25.2
9	**5.2**	**31.8**	**35.7**	**12.4**	**12.0**	**2.9**	8.1
Indopol 2100	**6.3**	**5.2**	**49.9**	**16.9**	**13.4**	**8.4**	14.7

*exo+couples

3.3. Comparing with a commercial sample

In the final section, the microstructure and end-use characteristic of the synthesized PIB from run 5 is assessed and compared with them of Indopol 2100, as a standard PIB. The GPC of the Indopol 2100 shows a number average molar mass of 4,300 g/mol and a polydispersity index of 2.3 which are almost identical with those of PIB from run 5. The total exo content of Indopol 2100 is 14.7 %, which is much higher than in the optimized sample (8.9 %, Table 2). In addition, both samples

revealed almost the same ^{13}CNMR spectrum (Figure 3), in which the main peaks had almost similar surface area. These observations affirm an almost identical microstructure of both polymers.

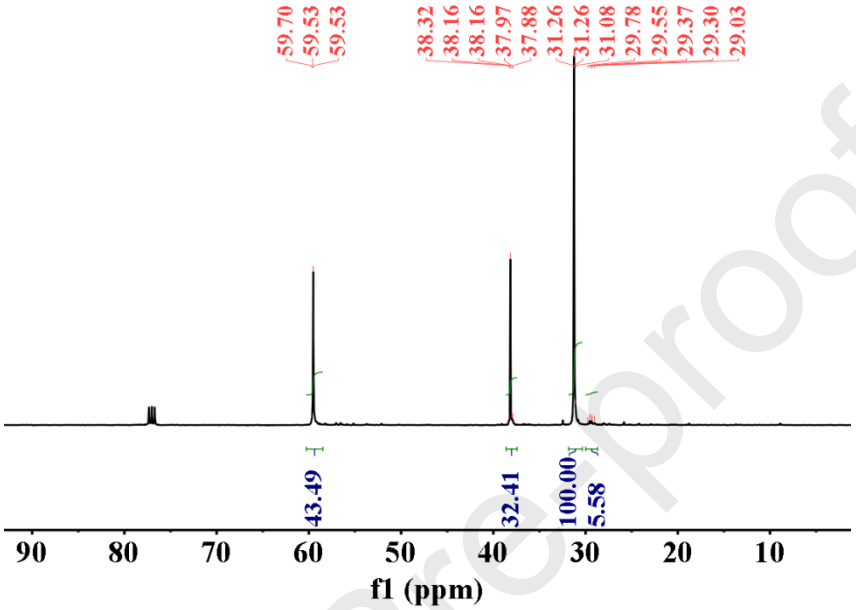

A

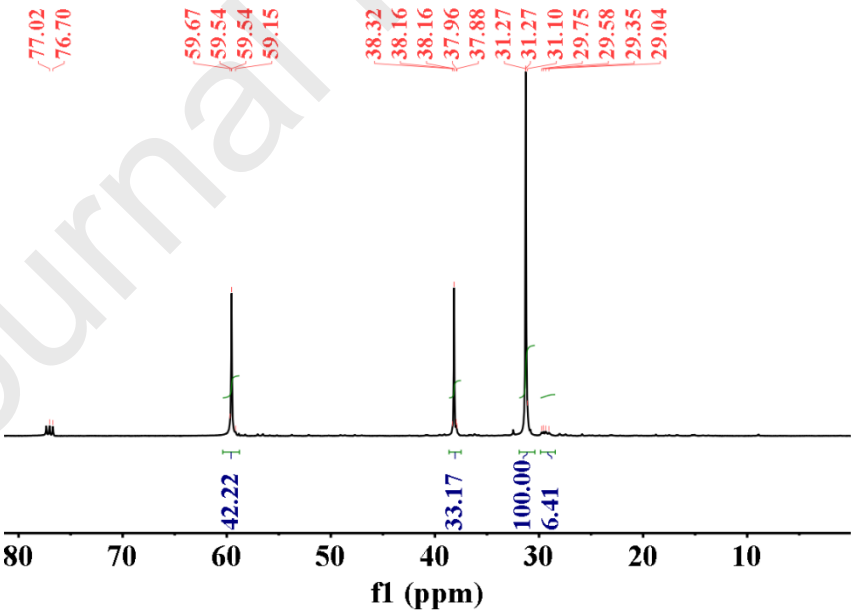

B

Figure 3. ^{13}CNMR spectra of A) commercial Indopol 2100 and B) synthesized PIB from S-IL catalyst (run 5 in Table 1).

Viscosity increase and viscosity index (VI) are the most important characteristics of a conventional grade PIB, which determine its efficiency in end-use application. They were obtained for a sample prepared by dissolving the synthesized PIB in base oil in 4 wt. % concentration. Notably, the synthesized PIB under optimal reaction conditions using S-IL (run 5 in Table 1) in the starting system formulation, revealed viscosity and VI increase of 170 and 7 cSt, respectively. According to the Indopol 2100 data sheet, a standard PIB should demonstrate viscosity and VI increase of at least 150 and 5 cSt, respectively. The outstanding performance of the synthesized PIB correlates with its microstructure, which was mainly originated by the presence of the S-IL precursor in the composition of the initiation system. In fact, this compound not only decreases the amount of corrosive $AlCl_3$, but also adapts the microstructure of PIB in order to achieve distinguished performance.

3.4. Characterization of S-IL

Due to the superior efficiency of the S-IL compound, in tailoring the as-synthesized PIB microstructure (suitable for viscosity improver applications) under mild reaction conditions, the structure of S-IL was analyzed by various techniques. The results obtained are discussed in this section.

To confirm the grafting of the ionic liquid moiety on the Hal surface and estimate its loading, TG analysis was employed. As shown in Figure 4, the comparison of the thermograms of pristine Hal and S-IL indicated that the two thermograms can be distinguished. More accurately, the Hal thermogram exhibited only two weight losses due to dehydration and dehydroxylation (T= 480

355 ºC), while in the S-IL thermogram an additional weight loss was recognized at T= 250 ºC (10 wt.
356 %) that is due to the degradation of the organic moiety and approve the grafting of the ionic liquid
357 moiety to Hal.

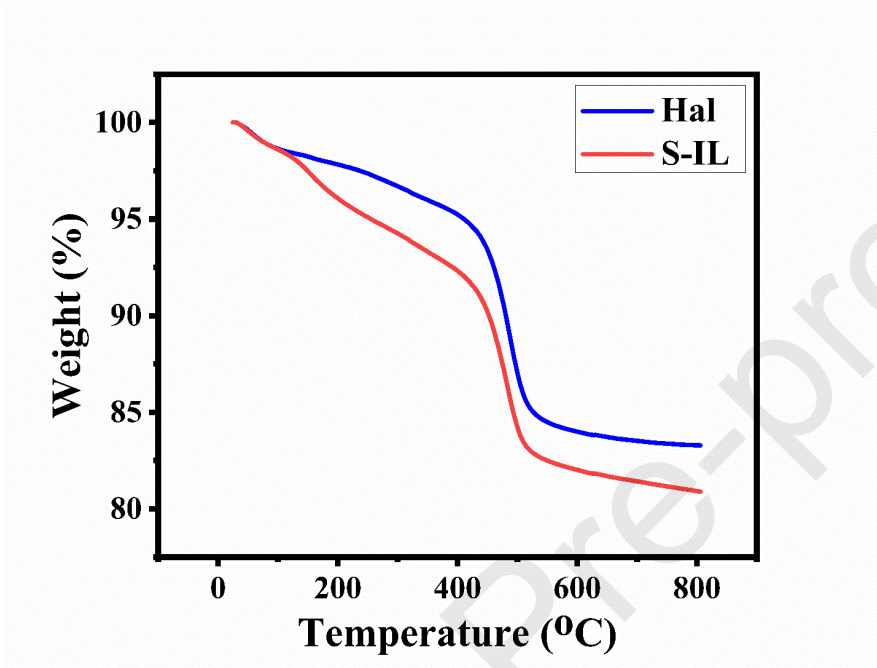

358

359 **Figure 4.** Thermograms of Hal and S-IL.

360 Since FTIR spectroscopy is also a potential technique to approve the conjugation of the organic
361 moiety to Hal, a comparison of the FTIR spectrum of Hal and S-IL was carried out. As shown in
362 Figure 5, the characteristic absorbance bands of Hal are observed at 535 cm^{-1} (Al-O-Si vibration),
363 1,037 cm^{-1} (Si-O stretching), 1,118 cm^{-1} (Si-O-Si stretching), 906 cm^{-1} (O-H deformation of
364 interior hydroxyl groups), 791 cm^{-1} (symmetric stretching of Si-O), and 745 cm^{-1} (stretching
365 vibrations of Si-O), 1,646 cm^{-1} (weak stretching and bending vibrations of H_2O molecules), 3,693
366 and 3,624 cm^{-1} (inner –OH groups) [69,70]. All the aforementioned absorbances are also discerned
367 in the FTIR spectrum of S-IL, confirming the fact that the Hal structure remained intact in the
368 course of ionic liquid grafting. It is worth noting that in the S-IL FTIR spectrum, the band observed

369 at 1,637 cm^{-1} is attributed to the –C=N bond, confirming the decoration of the Hal surface with
370 ionic liquid.

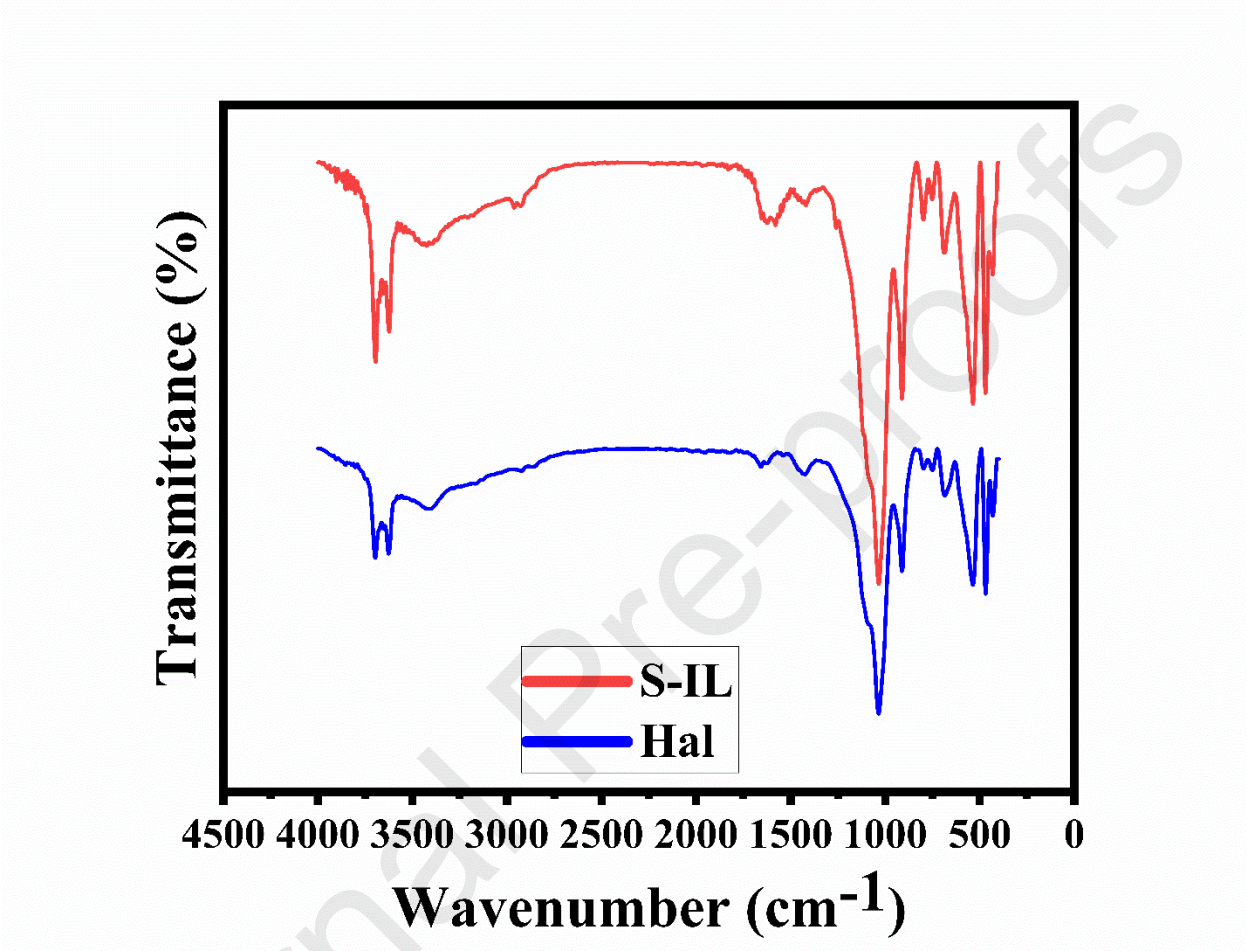

371

372 **Figure 5.** FTIR spectra of Hal and S-IL

373 To further elucidate the stability of the Hal structure after conjugation of ionic liquid and S-IL
374 formation, the XRD pattern of S-IL was recorded and compared with the pristine Hal pattern,
375 Figure 6. The XRD analysis of pristine Hal certified that the used Hal in this research did not
376 contain a specific impurity and its XRD pattern is in good agreement with the literature [69,70]
377 and showed the peaks at 2θ = 11.8, 19.9, 24.8, 26.5, 36.0, 38.5, 55.3 and 62.5° [71,72]. The S-IL
378 XRD pattern is identical to that of Hal, and the peaks that appeared in S-IL pattern showed no shift

379 compared to the characteristic bands of Hal, demonstrating the structural stability of Hal after ionic
380 liquid grafting.

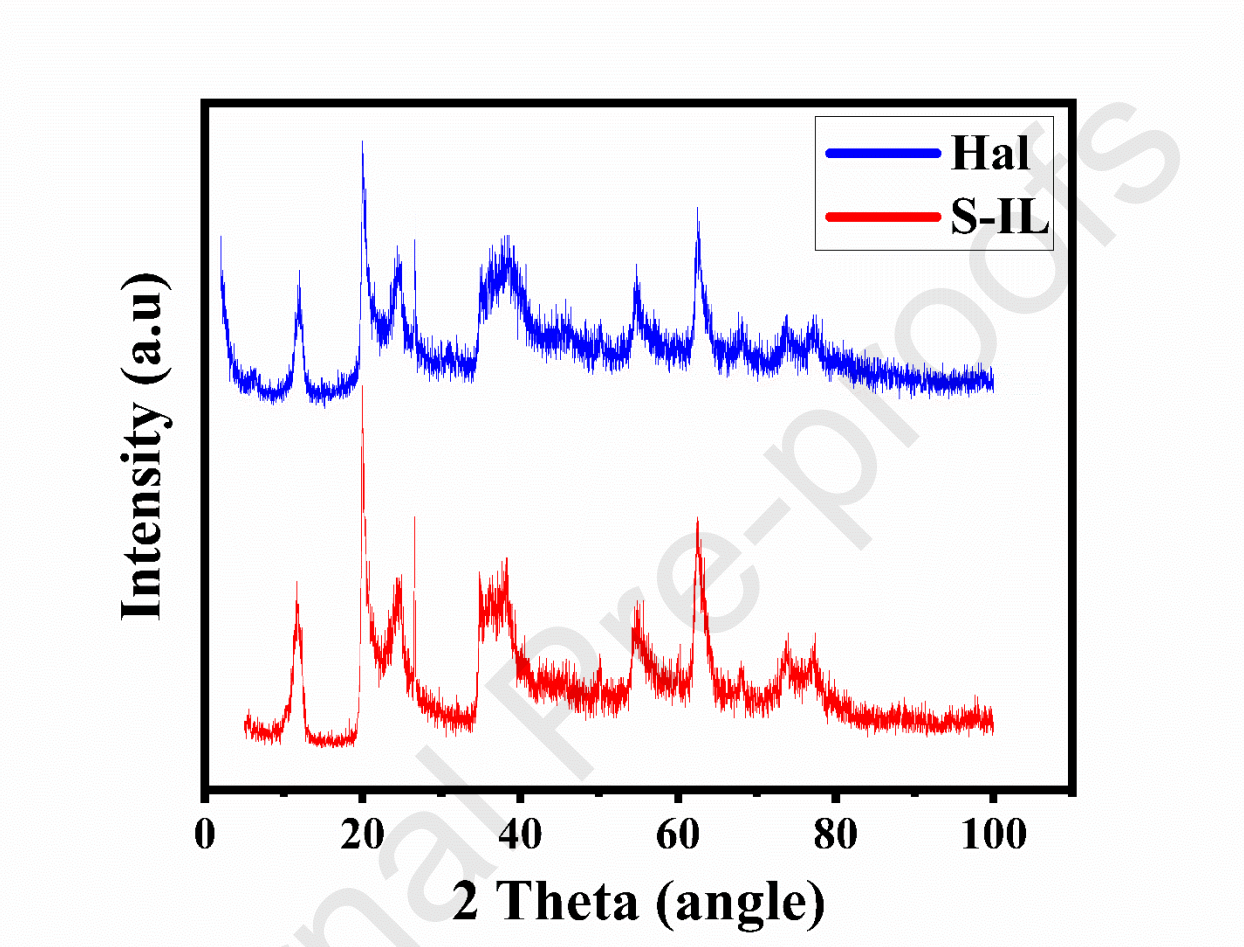

381

382 **Figure 6.** Comparison of XRD patterns of Hal and S-IL.

383 Elemental mapping analysis was performed to provide insight into the dispersion of the grafted
384 ionic liquid on the Hal surface. As illustrated in Figure 7, the elements detected in S-IL included,
385 Al, Si, O, N, C and Cl, among which Al, Si and O atoms are representative of the Hal framework,
386 while C, N and Cl are indicative of the ionic liquid grafted to Hal. Since the dispersion of all C, N
387 and Cl atoms is uniform, it can be concluded that the ionic liquid conjugated to Hal
388 homogeneously.

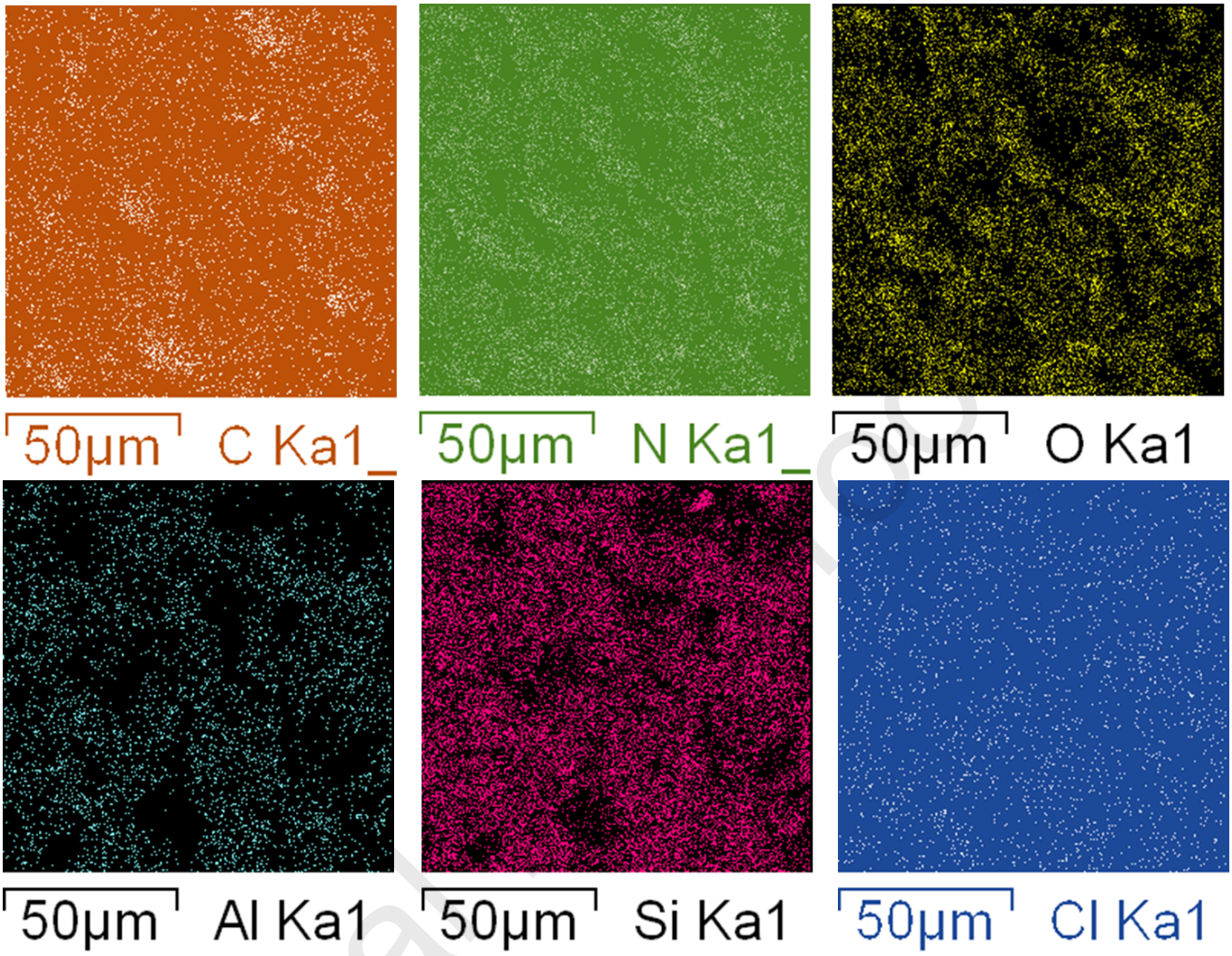

Figure 7. Elemental mapping analysis of S-IL.

Hal clay is known for its tubular morphology [73]. To investigate whether introduction of ionic liquid on the Hal alters its morphology, TEM images of S-IL were recorded. As it can be seen in Figure 8, S-IL also exhibited the tubular morphology, implying that the grafting of the ionic liquid did not result in morphological change. In fact, the stability of Hal structure was also confirmed by FTIR spectroscopy and XRD analysis.

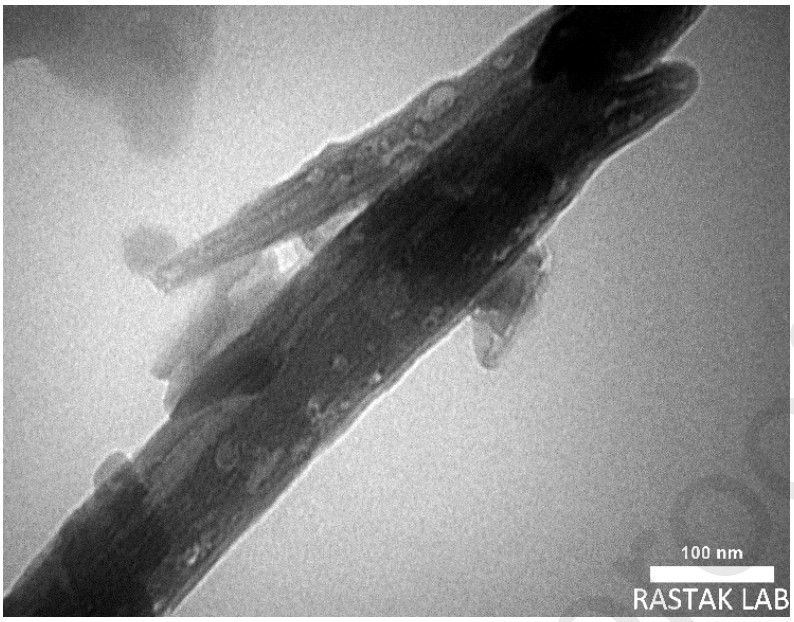

396

397 **Figure 8.** TEM image of S-IL.

398 To study the effect of grafting of IL on Hal, textural properties, *i.e.* specific surface area (S_{BET}),
399 total pore volume (V_P), and Average pore diameter (D_P) of Hal and S-IL were measured and
400 compared in Table 3. As shown, after introducing IL, the value of S_{BET} decreased from 62.6 to
401 51.9 m^2/g, indicating that IL covered the outer surface of the Hal. On the other hand, the value of
402 Vp also reduced from 14.3 to 11.9 cm^3/g, implying that the grafted organic moiety can also
403 penetrate into the Hal lumen. This issue can be further confirmed by decrement of the D_P value
404 from 8.1 to 3.1 nm.

405 **Table 3**. Textural properties of Hal and S-IL.

Sample	**S_{BET} (m^2/g)**	**V_P cm^3/g**	**D_P (nm)**
Hal	62.6	14.3	8.1
S-IL	51.9	11.9	3.1

406

3.5. Simulation Results

DFT calculations were reproduced synchronously for the systems IL, PIL, and S-IL, incorporating $AlCl_3$. This step denotes that the interaction is not thermodynamically favorable by 10.7 and 7.9 kcal/mol for IL and PIL, respectively, while S-IL is reversed, and goes towards exergonicity, and not by little, but by 17.6 kcal/mol. Here it is necessary to make the point that for the last system there is a factor to consider, that there is an interaction of the aluminum atom with an oxygen of the surface of the model of the halloysite (1.910 Å, see Figure 9) [42,74], simple compared to other past studies [75]. Starting from the dimer $(AlCl_3)_2$, which is the most real species [76], then the stability of the interaction is nearly the same for IL, with an unfavorable value of 10.1 kcal/mol, worsens a bit more for PIL till 11.8 kcal/mol, and finally for S-IL, the direct Al···O interaction is lost, and consequently another effect is that the dimer $(AlCl_3)_2$ ends up coming out of the cleft between the ionic liquid part of the S-IL and its halloysite moiety. Anyway, the destabilization is only of 5.7 kcal/mol. Therefore, the symbiosis between the aluminum catalyst and the S-IL is more accessible than for IL or PIL. This could help to explain why S-IL has a different and/or somewhat better performance, but also explains that the ration $AlCl_3$/IL must increase for the S-IL system since some aluminium centers will be trapped by the hydroxyl groups once the $AlCl_3$ dimer is broken, killing or slowing down their activity as active catalytic centers.

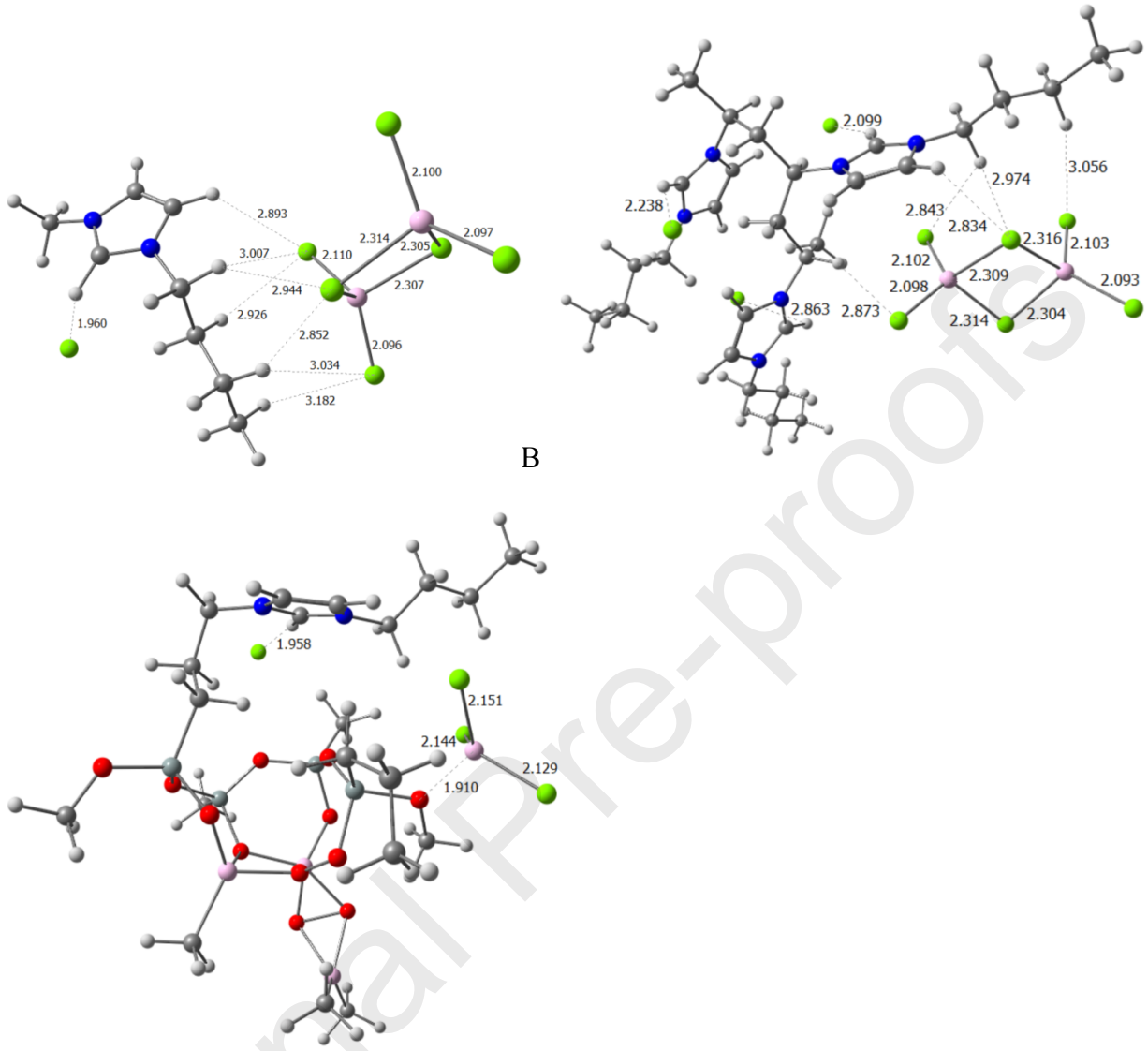

425 A B

426 C

427 **Figure 9.** DFT optimized structures of the interaction of $(AlCl_3)_2$ with A: IL, B: PIL, and for
428 $AlCl_3$ with C: S-IL (selected distances given in Å).

429 With the action of an ethanol molecule, the aluminum would then be hydroxylated, presenting
430 values of 13.2, 15.0 and 16.8 kcal/mol for IL, PIL and S-IL, respectively. These values are
431 unusually relatively unstable, but if again we also treat with a dimer of $AlCl_3$, once cleaved,
432 causing the remaining $AlCl_3$ to stabilize forming the anion $AlCl_4^-$, thanks to a chlorine of the ionic
433 liquid, this step causes the catalyst to pass from the endergonicity of $AlCl_3$, monomeric or dimeric,

to exergonicity. Thus, favorable values of -15.7 and -17.0 and -16.3 kcal/mol are achieved for IL, PIL, and S-IL, respectively. Although S-IL achieves a synchrony for this last studied hydroxylated anionic species, with respect to the other 2 systems, IL and PIL, it should be mentioned that again the aluminium catalytic moiety skips from the cavity between the ionic liquid moiety and the halloysite.

Additional analyses on the sterical hindrance that the Hal system produces on the metal center unveils that the occupation by means of the $\%V_{Bur}$, calculated with the SambVca2.1 package [77]. increases from 39.6 to 48.8 % (see the steric maps in Figure 10). Even though it may seem a significant change, dividing by quadrants, the change is attributed only to one quadrant (71.4%), whereas the other three range from 40.4 to 42.2 %.

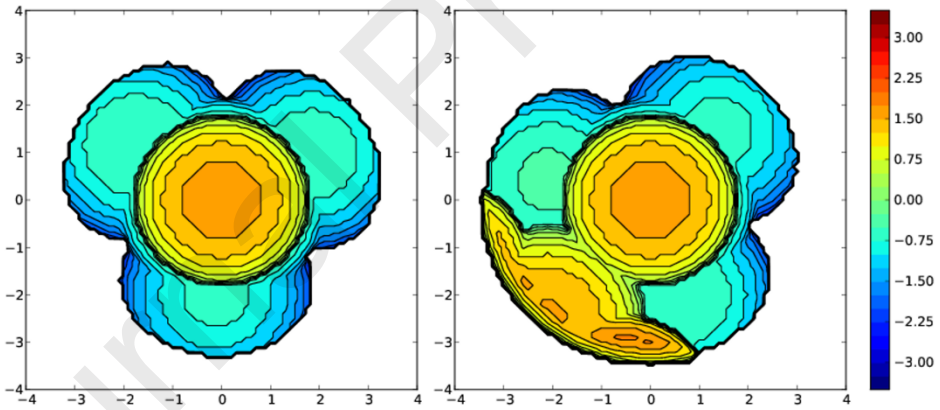

Figure 10. Steric maps (xy plane) of the hydroxylated aluminium species without (left) and with Hal (right); with the center on the oxygen, the z axis crossing the Al-O bond, and the xy plane parallel by the plane defined by the three chloride atoms; curves are given in Å.

449 The interaction of the aluminum catalyst with the three ionic liquids is neither covalent nor ionic
450 in nature, but through weak interactions, and therefore an analysis was carried out through the non-
451 covalent interaction (NCI) plots. Thus, Figure 11 demonstrates the great importance of this type
452 of interaction. The NCI plots were calculated using the NCI plot program developed by Contreras-
453 García et al. [78,79], at the BP86-D3/Def2SVP level of theory [80]. In particular, starting with the
454 simplest system, IL, the interaction of the $(AlCl_3)_2$ catalyst occurs between the butyl chain and
455 three chlorine atoms (Figure 11a). Thus, when hydroxyl is present, the interaction is identical, as
456 this chemical group is located as far as possible from this butyl chain (Figure 11b). Going to the
457 more complex PIL and S-IL systems, the same conclusions can be extrapolated, but it is necessary
458 to add NCI interactions specific to the structures themselves, for example, between the chlorine
459 which defines the nature of the liquid ionic, with a butyl chain, but also with the others in the case
460 of the PIL (Figure 11c), or with the complex framework of the S-IL (Figure 11d). For more details
461 on all systems, see SI, Table S1. In addition, the Natural Bond Orbital (NBO) charge on the
462 aluminium for the complexes with the $(AlCl_3)_2$ dimer is more positive in average for IL (1.265)
463 than PIL (PIL (1.257) and S-IL (1.260). These NBO charges then show asynchrony between both
464 aluminium centers when bonding the hydroxyl group, with an increase of the positive charge on
465 the aluminium that allocates this group. For IL (1.418) and even more for PIL (1.406) the values
466 are slightly less positive than for S-IL (1.421). However, to explain reactivity future mechanistic
467 studies will be necessary to evaluate the whole mechanism of polymerization reaction [81], not
468 only to understand the action of each liquid ionic, but also simply to understand the mechanism,
469 and thus be able to rationalize the major or minor dimension of the chains formed. But this will
470 need to be combined with more complementary experimental results, as the current differences are
471 of a magnitude that would not allow general conclusions to be reached.

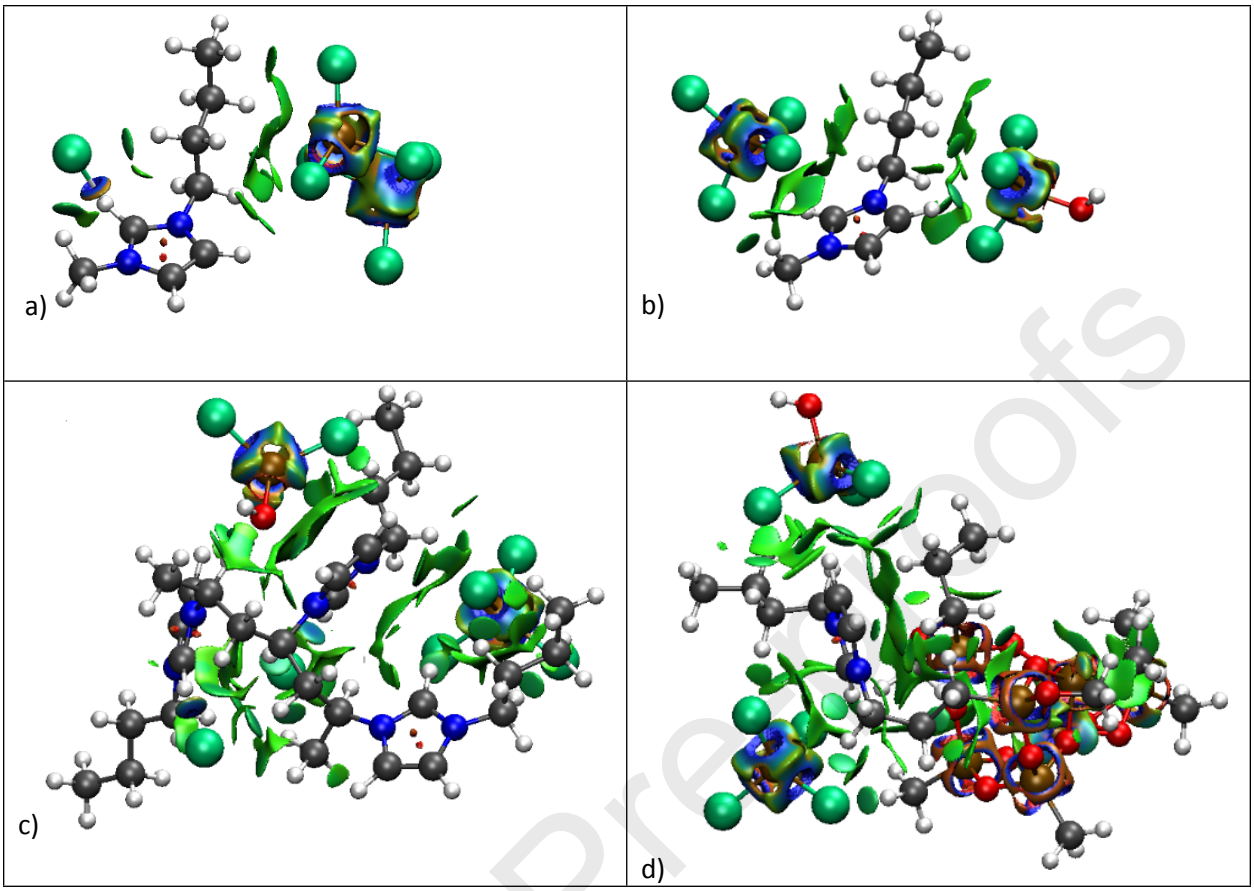

Figure 11. NCI plots for a) IL-$(AlCl_3)_2$, b) IL-$(AlCl_3)_2OH^-$, c) PIL-$(AlCl_3)_2OH^-$ and d) S-IL-$(AlCl_3)_2OH^-$.

Conclusions

To decrease the loading of corrosive $AlCl_3$ cationic initiator and tune the polymerization conditions in order to reach a safer and more economical process, different systems containing ionic liquids of various natures, including IL, PIL and S-IL were synthesized and have been employed as the main initiator ingredients in the cationic polymerization of isobutylene monomer. In particular, S-IL resulted PIB suitable for conventional grade applications under optimized moderate reaction conditions, *i.e.* T = 0 °C, compared to neat $AlCl_3$. The synthesized PIB demonstrated comparable

characteristic to Indopol 2100, represented as commercial conventional grade PIB by Ineos, in VI improving applications. This is a great achievement in the production of this type of PIB with favorable characteristics, not only because of the moderate polymerization condition, but also due to decrement of the required content of corrosive $AlCl_3$ initiator. In addition, DFT calculations were performed to deepen the importance of the interaction between the 3 different systems studied (IL, PIL and SIL) and the catalytic system $AlCl_3$, and subsequently hydroxylated with the alcoholic substrate. The results obtained by molecular simulation supported the experimentally obtained advances towards a better performance of the S-IL/$AlCl_3$ initiator.

CRediT authorship contribution statement

Saleh Yousefi, Michele Tomasini: Investigation. Mehdi Nekoomanesh, Mehrsa Emami, Eduard Bardají: Investigation, Supervision, Formal analysis. Samahe Sadjadi, Naeimeh Bahri-Laleh, Albert Poater: Supervision, Conceptualization.

Conflicts of interest

There is no conflict to declare.

Acknowledgements

The authors are thankful to Iran Polymer and Petrochemical Institute for financial support. Albert Poater is a Serra Húnter Fellow and ICREA Academia Prize 2019, and thanks the Spanish Ministerio de Ciencia e Innovación for projects PID2021-127423NB-I00 and PGC2018-097722-B-I00.

References

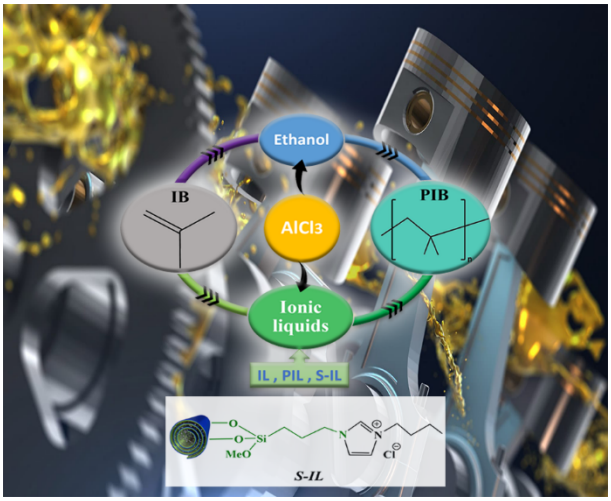

Highlights

- $AlCl_3$ supported on functionalized halloysite with a ionic liquid as a catalyst.
- Synthesis of ionic liquids to support $AlCl_3$ and experimental and DFT calculations characterization
- Synthesis of polyisobutylene.
- Experimental mild conditions together with excellent catalytic activity.

Conflict of Interest

There are no conflicts of interest

CRediT authorship contribution statement

517 Saleh Yousefi, Michele Tomasini: Investigation. Mehdi Nekoomanesh, Mehrsa Emami, Eduard Bardají:

518 Investigation, Supervision, Formal analysis. Samahe Sadjadi, Naeimeh Bahri-Laleh, Albert Poater:

519 Supervision, Conceptualization.

520

521

[1] A. Rahbar, N. Bahri-Laleh, M. Nekoomanesh-Haghighi, Fuel 302 (2021) 121111.
[2] F.T. Hong, V. Ladelta, R. Gautam, S.M. Sarathy, N. Hadjichristidis, ACS Appl. Polym. Mater. 3 (2021) 3811.
[3] T. Rajasekhar, G. Singh, G.S. Kapur, S.S.V. Ramakumar, RSC Adv. 10 (2020) 18180.
[4] K. Tekin, S. Ucar, S. Karagöz, Energy Fuels 33 (2019) 11101.
[5] J.E. Ruffell, T.J. Farmer, D.J. Macquarrie, M.S. Stark, Ind. Eng. Chem. Res. 58 (2019) 19649.
[6] A. Ribas-Massonis, M. Cicujano, J. Duran, E. Besalú, A. Poater, Polymers 14 (2022) 2856.
[7] A. Hanifpour, N. Bahri-Laleh, A. Mohebbi, M. Nekoomanesh-Haghighi, Iran. Polym. J. 31 (2022) 107.
[8] M. N. Vo, M. Call, C. Kowall, J.K. Johnson, Effect of Chain Length on the Dipole Moment of Polyisobutylene Succinate Anhydride, Ind. Eng. Chem. Res. 61 (2022) 2359.
[9] S. Deng, H. Tian, D. Sun, S. Liu, Q. Zhao, J. Polym. Res. 27 (2020) 55.
[10] S. Müller, M. Hackett, M. Yoneyama, W. Yang, IHS Report: LUBRICATING OIL ADDITIVES, 2012.
[11] B. Yang, R. F. Storey, React. Funct. Polym. 150 (2020) 104563.
[12] Q. Huang, P. He, J. Wang, Y.-x. Wu, Chin. J. Polym. Sci. 31 (2013) 1139.
[13] J.B. Alves, M.K. Vasconcelos, L.H.R. Mangia, M. Tatagiba, J. Fidalgo, D. Campos, P.L. Invernici, M. V. Rebouças, M.H.S. Andrade, J.C. Pinto, Processes 9 (2021) 1315.
[14] W. Sien Fong, Polybutene polymers. In SRI Report, No. 74. California, USA, 1971.
[15] Y.-B. Jia, Y.-B.; Wang, W.-M. Ren, T. Xu, J. Wang, X.-B. Lu, Macromolecules 47 (2014) 1966.
[16] Q. Liu, Y.-X. Wu, Y.-X. Wu Y. Zhang, P.-F. Yan, R.-W. Xu, Polymer 51 (2010) 5960.
[17] S. Karimi, S. Sadjadi, N. Bahri-Laleh, M. Nekoomanesh-Haghighi, Mol. Catal. 509 (2021) 111648.
[18] J.M. Hogg, F. Coleman, A. Ferrer-Ugalde, M.P. Atkins, M. Swadzba-Kwasny, Liquid coordination complexes: a new class of Lewis acids as safer alternatives to BF_3 in synthesis of polyalphaolefins, Green Chem. 17 (2015) 1831.
[19] J.M. Hogg, A. Ferrer-Ugalde, F. Coleman, M. Swadźba-Kwaśny, ACS Sustainable Chem. Eng. 7 (2019) 15044.
[20] Z. Lei, B, Chen, Y.-M. Koo, D.R. MacFarlane, Chem Rev. 117 (2017) 6633.
[21] L. Cao, H.W. Kim, Y.J. Jeong, S.C. Han, J.K. Park, Org. Process. Res. Dev. 26 (2022) 207.
[22] G. Lazzara, G. Cavallaro, A. Panchal, R. Fakhrullin, A. Stavitskaya, V. Vinokurov, Y. Lvov, Curr. Opin. Colloid Interface Sci. 35 (2018) 42.
[23] G. Cavallaro, L. Chiappisi, P. Pasbakhsh, M. Gradzielski, G. Lazzara, Appl. Clay Sci. 160 (2018) 71.
[24] L. Deng, P. Yuan, D. Liu, P. Du, J. Zhou, Y. Wei, Y. Song, Y. Liu, Appl. Clay Sci. 181 (2019) 105240.
[25] V. Vinokurov, A. Stavitskaya, A. Glotov, A. Ostudin, M. Sosna, P. Gushchin, Y. Darrat, Y. Lvov, J. Solid State Chem. 268 (2018) 182.
[26] R.J. Smith, K.M. Holder, S. Ruiz, W. Hahn, Y. Song, Y.M. Lvov, J.C. Grunlan, Adv. Funct. Mater. 28 (2018) 1703289.
[27] G. Cavallaro, G. Lazzara, S. Milioto, F, Parisi, Halloysite Nanotubes for Cleaning, Chem. Rec. 18 (2018) 1.

[30] L.-L. Deng, P. Yuan, D. Liu, F. Annabi-Bergaya, J. Zhou, F. Chen, Z. Liu, Appl. Clay Sci. 143 (2017) 184.
[31] Y. Wei, P. Yuan, D. Liu, D. Losic, D. Tan, F. Chen, H. Liu, J. Zhou, P. Du, Y. Song, Chem. Commun. 55 (2019) 2110.
[32] M. Massaro, G. Lazzara, S. Milioto, R. Noto, S. Riela, J. Mater. Chem. B 5 (2017) 2867.
[33] M. Massaro C.G. Colletti, G. Buscemi, S. Cataldo, S. Guernelli, G. Lazzara, L.F. Liotta, F. Parisi, A. Pettignano, S. Riela, New J. Chem. 42 (2018) 13938.
[34] S. Dehghani, S. Sadjadi, N. Bahri-Laleh, M. Nekoomanesh-Haghighi, A. Poater, Appl. Organomet. Chem. 33 (2019) e4891.
[35] Z. Zhu, D. Ding, Y. Zhang, Y. Zhang, Appl. Clay Sci. 196 (2020) 105761.
[36] M. Massaro, C.G. Colletti, B. Fiore, V. La Parola, G. Lazzara, S. Guernelli, N. Zaccheroni, S. Riela, Appl. Organomet. Chem. 33 (2019) e4665.
[37] M.J. Baruah, T.J. Bora, R. Dutta, S. Roy, A.K. Guha, K.K. Bania, Mol. Catal. 515 (2021) 111858.
[38] A. Mahajan, P. Gupta, New J. Chem. 44 (2020) 12897.
[39] J. Jin, J. Ouyang, H. Yang, Nanoscale Res. Lett. 12 (2017) 240.
[40] C. Lin, P. Ying, M. Huang, P. Zhang, T. Yang, G. Liu, T. Wang, J. Wu, V. Levchenko, J. Polym. Res. 28 (2021) 375.
[41] Y. Huo, H. Ge, C. Lin, P. Ying, M. Huang, P. Zhang, T. Yang, G. Liu, J. Wu, V. Levchenko, Appl. Compos. Mater. 29 (2022) 729.
[42] S. Sadjadi, F. Koohestani, G. Pareras, M. Nekoomanesh-Haghighi, N. Bahri-Laleh, A. Poater, J. Mol. Liq. 331 (2021) 115740.
[43] Gaussian 16, Revision C.01, M.J. Frisch, G.W. Trucks, H.B. Schlegel, G.E. Scuseria, M.A. Robb, J.R. Cheeseman, G. Scalmani, V. Barone, G.A. Petersson, H. Nakatsuji, X. Li, M. Caricato, A.V. Marenich, J. Bloino, B.G. Janesko, R. Gomperts, B. Mennucci, H.P. Hratchian, J.V. Ortiz, A.F. Izmaylov, J.L. Sonnenberg, D. Williams-Young, F. Ding, F. Lipparini, F. Egidi, J. Goings, B. Peng, A. Petrone, T. Henderson, D. Ranasinghe, V.G. Zakrzewski, J. Gao, N. Rega, G. Zheng, W. Liang, M. Hada, M. Ehara, K. Toyota, R. Fukuda, J. Hasegawa, M. Ishida, T. Nakajima, Y. Honda, O. Kitao, H. Nakai, T. Vreven, K. Throssell, J.A. Montgomery, Jr., J.E. Peralta, F. Ogliaro, M.J. Bearpark, J.J. Heyd, E.N. Brothers, K.N. Kudin, V.N. Staroverov, T.A. Keith, R. Kobayashi, J. Normand, K. Raghavachari, A.P. Rendell, J.C. Burant, S.S. Iyengar, J. Tomasi, M. Cossi, J.M. Millam, M. Klene, C. Adamo, R. Cammi, J.W. Ochterski, R.L. Martin, K. Morokuma, O. Farkas, J.B. Foresman, D.J. Fox, Gaussian, Inc., Wallingford CT, 2016.
[44] A. D. Becke, Phys. Rev. A 38 (1988) 3098.
[45] J.P. Perdew, Phys. Rev. B 33 (1986) 8822.
[46] S. Grimme, J. Antony, S. Ehrlich, H. Krieg, J. Chem. Phys. 132 (2010) 154104.
[47] F. Weigend, R. Ahlrichs, Phys. Chem. Chem. Phys. 7 (2005) 3297.
[48] F. Weigend, Phys. Chem. Chem. Phys. 8 (2006) 1057.
[49] A. V. Marenich, C.J. Cramer, D.G. Truhlar, J. Phys. Chem. B 113 (2009) 6378.
[50] A.D. Becke, J. Chem. Phys. 98 (1993) 5648.
[51] P.J. Stephens, F.J. Devlin, C.F. Chabalowski, M.J. Frisch, J. Phys. Chem. 98 (1994) 11623.
[52] C.T. Lee, W.T. Yang, R.G. Parr, Phys. Rev. B 37 (1988) 785.
[53] F. Ferrante, N. Armata, G. Lazzara, J. Phys. Chem. C 121 (2017) 2951.
[54] S. Sadjadi, N. Bahri-Laleh, J. Porous Mater. 25 (2018) 821.
[55] A. Shams, S. Sadjadi, J. Duran, S. Simon, A. Poater, N. Bahri-Laleh, Appl. Organomet. Chem. (2022) e6719.
[56] M. Tabrizi, N. Bahri-Laleh, S. Sadjadi, M. Nekoomanesh-Haghighi, J. Mol. Liq. 335 (2021) 116299.
[57] M. Mashayekhi, S. Talebi, S. Sadjadi, N. Bahri-Laleh, Appl. Catal. A: Gen. 623 (2021) 118274.

[58] S. Karimi, N. Bahri-Laleh, S. Sadjadi, G. Pareras, M. Nekoomanesh-Haghighi, A. Poater, J. Ind. Eng. Chem. 97 (2021) 441–451.
[59] M. Tabrizi, S. Sadjadi, G. Pareras, M. Nekoomanesh-Haghighi, N. Bahri-Laleh, A. Poater, J. Colloid Interface Sci. 581 (2021) 939.
[60] S. Dehghani, S. Sadjadi, N. Bahri-Laleh, M. Nekoomanesh-Haghighi, A. Poater, Appl. Organomet. Chem. 33 (2019) e4891.
[61] N. Bahri-Laleh, S. Sadjadi, A. Poater, J. Colloid Interface Sci. 531 (2018) 421.
[62] F. Nouri-Ahangarani, N. Bahri-Laleh, M. Nekomanesh Haghighi, M. Karbalaei, Des Monomers Polym. 19 (2016) 394.
[63] S. Shirbakht, S.A. Mirmohammadi, K. Didehban, S. Sadjadi, N. Bahri-Laleh, Adv. Polym. Technol. 37 (2018) 2588.
[64] M.S. Abbas-Abadi, R. Rashedi, A. Sepahi, L. Heydari, A. Farhadi, M. Biglarkhani, Iran. Polym. J. 29 (2020) 659.
[65] G. Zhu, L. Wang, J. Kuang, G. Xu, Y. Zhang, Q. Wang, Macromolecules 54 (2021) 6109.
[66] D.I. Shiman, I.V. Vasilenko, S.V. Kostjuk, Polymer 54 (2013) 2235.
[67] Q. Liu, Y. Wu, P. Yan, Y. Zhang, R. Xu, Macromolecules 44 (2011) 1866.
[68] I. Puskas, E.M. Banas, A.G. Nerheim, J. Polym. Sci., C Polym. Symp. 56 (1976) 191.
[69] S. Mahmoudi-Gom Yek, T. Baran, M. Nasrollahzadeh, R. Bakhshali-Dehkordi, Nuray Yılmaz Baran, M. Shokouhimehr, Optik 238 (2021) 166672.
[70] N. Yılmaz Baran, T. Baran, A. Menteş, Appl. Clay Sci. 181 (2019) 105225.
[71] H. Zhu, M.L. Du, M.L. Zou, C.S. Xu, Y. Q. Fu, Dalton Trans. 41 (2012) 10465.
[72] P. Yuan, P.D. Southon, Z. Liu, M.E.R. Green, J.M. Hook, S.J. Antill, C.J. Kepert, J. Phys. Chem. C 112 (2008) 15742.
[73] S. Sadjadi, Appl. Clay Sci. 189 (2020) 105537.
[74] N. Bahri-Laleh, S. Sadjadi, M. M. Heravi, M. Malmir, Appl. Organomet. Chem. 2 (2018) e4283.
[75] F. Ferrante, N. Armata, G. Lazzara, J. Phys. Chem. C 119 (2015) 16700.
[76] M. Fallah, N. Bahri-Laleh, K. Didehban, A. Poater, Appl. Organomet. Chem. 34 (2020) e5333.
[77] L. Falivene, Z. Cao, A. Petta, L. Serra, A. Poater, R. Oliva, V. Scarano, L. Cavallo, Nat. Chem. 11 (2019) 872.
[78] E.R. Johnson, S. Keinan, P. Mori-Sanchez, J. Contreras-Garcia, A.J. Cohen, W.T. Yang, J. Am. Chem. Soc. 132 (2010) 6498.
[79] J. Contreras-Garcia, E.R. Johnson, S. Keinan, R. Chaudret, J.P. Piquemal, D.N. Beratan, W.T. Yang, J. Chem. Theory Comput. 7 (2011) 625.
[80] J. Poater, M. Gimferrer, A. Poater, Inorg. Chem. 57 (2018) 6981.
[81] N. Bahri-Laleh, A. Hanifpour, S.A. Mirmohammadi, A. Poater, M. Nekoomanesh-Haghighi, G. Talarico, L. Cavallo, Prog. Polym. Sci. 84 (2018) 89.